Journal of ELECTRONIC MATERIALS
DOI: 10.1007/s11664-016-5161-6

Quantum Molecular Dynamical Calculations of PEDOT 12-Oligomer and its Selenium and Tellurium Derivatives

AMINA MIRSAKIYEVA ,[1,6] HÅKAN W. HUGOSSON,[1,4] XAVIER CRISPIN,[5] and ANNA DELIN[1,2,3]

1.—Material and Nanophysics Department, KTH Royal Institute of Technology, 164 40 Kista, Sweden. 2.—Swedish e-Science Research Center, KTH, 10044 Stockholm, Sweden. 3.—Department of Physics and Astronomy, Uppsala University, Box 516, 751 20 Uppsala, Sweden. 4.—Department of Electronics, Mathematics and Natural Sciences, University of Gävle, Gävle, Sweden. 5.—Laboratory of Organic Electronics, Department of Science and Technology, Linköping University, 601 74 Norrköping, Sweden. 6.—e-mail: aminami@kth.se

We present simulation results, computed with the Car–Parrinello molecular dynamics method, at zero and ambient temperature (300 K) for poly(3,4-ethylenedioxythiophene) [PEDOT] and its selenium and tellurium derivatives PEDOS and PEDOTe, represented as 12-oligomer chains. In particular, we focus on structural parameters such as the dihedral rotation angle distribution, as well as how the charge distribution is affected by temperature. We find that for PEDOT, the dihedral angle distribution shows two distinct local maxima whereas for PEDOS and PEDOTe, the distributions only have one clear maximum. The twisting stiffness at ambient temperature appears to be larger the lighter the heteroatom (S, Se, Te) is, in contrast to the case at 0 K. As regards point charge distributions, they suggest that aromaticity increases with temperature, and also that aromaticity becomes more pronounced the lighter the heteroatom is, both at 0 K and ambient temperature. Our results agree well with previous results, where available. The bond lengths are consistent with substantial aromatic character both at 0 K and at ambient temperature. Our calculations also reproduce the expected trend of diminishing gap between the highest occupied molecular orbital and the lowest unoccupied molecular orbital with increasing atomic number of the heteroatom.

Key words: PEDOT, PEDOS, PEDOTe, tellurium, density functional theory, dihedral angle

INTRODUCTION

Poly(3,4-ethylenedioxythiophene) (PEDOT) is a conducting polymer with wide technological use in, e.g., organic transistors, photovoltaic devices, displays, and biosensors. It has also recently received increasing attention as a thermoelectric material since it exhibits a number of attractive features for such applications—it is stable in air, solution-processable to create patterns on large areas, easily synthesized, flexible, and environmentally friendly. Indeed, PEDOT doped with polystyrene sulfonate (PEDOT:PSS) has been demonstrated to have a relatively high figure of merit zT.[1–3] Important properties of PEDOT, e.g., the degree of aromaticity (see Fig. 1), band gap, charge distribution, and transport properties, depend on the conformation of the polymer. At finite temperature, PEDOT is not planar. Instead, the EDOT monomers rotate around their equilibrium positions, with the dihedral angle constantly changing. This results in a statistical distribution of the dihedral angle for a macroscopic sample. The observed electronic properties of a macroscopic PEDOT film can be expected to depend on this dihedral angle distribution, among other things. It is, therefore, of special interest to perform simulations at ambient temperature for these systems.

(Received May 27, 2016; accepted November 18, 2016)

Published online: 02 December 2016

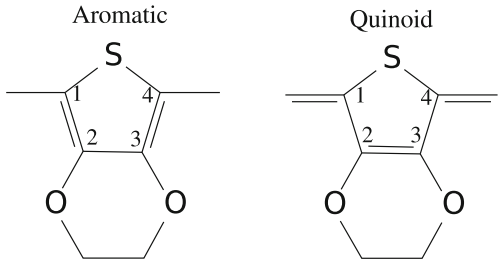

Fig. 1. EDOT monomer in aromatic conformation (left) and quinoid conformation (right). In the aromatic conformation, the double bonds form between carbon atoms 1 and 2, and between carbon atoms 3 and 4. In the quinoid conformation, the double bonds instead form between carbon atoms 2 and 3, and between monomers. Carbon atoms forming double bonds can be recognized through shorter bond lengths and, possibly, also by a higher number of electrons relative to other carbon atoms. A perfect single (double) bond is expected to be 1.54 (1.34 Å).

In addition to the technological applications mentioned above, conducting polymers such as PEDOT are also relevant for spintronics and spincaloritronics applications.[4] In this context, the inverse spin Hall effect (ISHE) is of special interest as the main read-out mechanism for the spin Seebeck effect. Since the ISHE depends sensitively on the spin–orbit coupling, it is of relevance to investigate conducting polymers containing atoms with large spin–orbit coupling.

In this work, we present a theoretical investigation, using computational methods based on density functional theory (DFT), of the geometrical structure and charge distribution at ambient temperature of neutral PEDOT and its derivatives PEDOS and PEDOTe, i.e., derivatives where the sulfur atoms have been replaced by selenium and tellurium, respectively. Our calculations pertain to straight 12-oligomer chains, where we, in particular, focus our attention to the six central monomers to avoid edge effects.

From an experimental point of view, direct measurement of the electronic and structural properties of pristine PEDOT is challenging—the films usually have a complex network morphology, with dopants as well as solvents present. High-precision calculations are, therefore, especially useful to obtain a basic understanding of the fundamental structural and electronic properties of these polymers. Our results for PEDOTe serve at this point as theoretical predictions since this system, to the best of our knowledge, has not yet been successfully synthesized.

COMPUTATIONAL DETAILS

The ground-state structure optimization as well as the finite-temperature quantum molecular dynamical simulations were carried out using the Car–Parrinello molecular dynamics (CPMD) method.[5,6] This method treats all atoms of the system quantum mechanically at the DFT level. The interatomic forces are calculated at each time step, keeping the electron orbital functions close to the Born–Oppenheimer surface with the help of fictitious dynamics. In the present calculations, we used a fictitious electron mass of 800 atomic units and a time step of $\Delta t = 0.1$ fs to integrate the equations of motion. We employed the BLYP[7,8] approximation to the exchange–correlation part of the total energy functional. It is well-established that this functional gives sound results for undoped PEDOT.[10] Doped systems require another approach, however. In the present work, we address only the undoped situation. The effect of the core electrons was described using Troullier–Martins norm-conserving pseudopotentials[9] and the valence electron wave functions were expanded in a plane-wave basis set with a kinetic cut-off of 90 Ry. The initial configuration was chosen to be planar, with atomic distances taken from the earlier studies by Kim and Brédas.[10] The minimum distance between adjacent polymers (from edge to edge) was set to 11 Å, corresponding to a unit cell parameter of about 20 Å. In order to check that this distance was indeed sufficient to avoid polymer–polymer interactions, we performed test calculations for several distances ranging from 6 Å to 11 Å, which all gave equivalent results. From this initial guess, the ground-state structure was found through quenching and annealing. The system was subsequently equilibrated during 2.5 ps. In this step, the temperature was controlled by rescaling the velocities so as to keep the system within a 40-K tolerance window around 300 K. After equilibration, followed an MD run of 12 ps at 300 K, during which statistics were collected. Here, temperature control was implemented for both the ionic and electronic degrees of freedom using Nosé–Hoover thermostats[11,12] with a characteristic frequency of 10,000 cm^{-1} for the electrons and 480 cm^{-1} for the ions. All calculations pertain to 12-oligomers. In order to extract data relevant for the corresponding polymer (in principle, an infinitely long chain), we have focused our analysis to the computed data for the 6 middle monomers in the 12-oligomer, thereby avoiding edge effects.

RESULTS

The bond lengths in the carbon backbone are relevant for analyzing the degree of aromatic/quinoid character in these systems. Our computed bond lengths (see Fig. 2) reveal that all three studied polymers exhibit substantial aromaticity in the ground state as well as at ambient temperature, with two short bonds and one long bond within each monomer carbon backbone. The bonds between consecutive monomers are long, indicating single bonds (not shown). The difference between long and short bonds is smallest in PEDOT, and largest in PEDOTe. At ambient temperature, the carbon backbone bond lengths in all three systems are slightly larger compared to the ground state. We

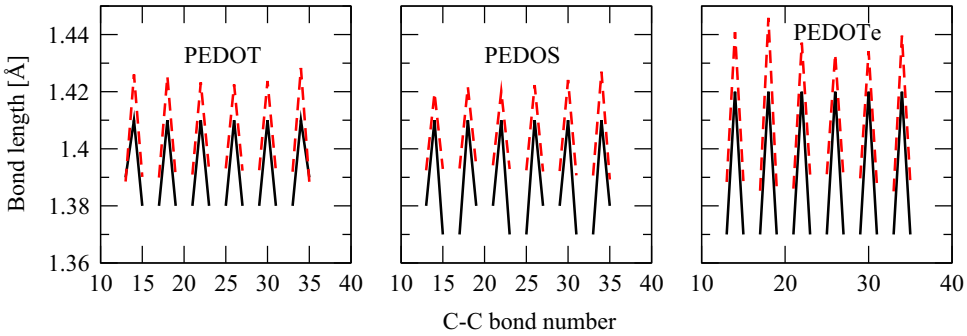

Fig. 2. (Color online) Carbon backbone bond lengths within monomers 4–9 of the 12-oligomer, at 0 K (black full lines) and 300 K (red dashed lines). The first three and last three monomers are not included to avoid edge effects.

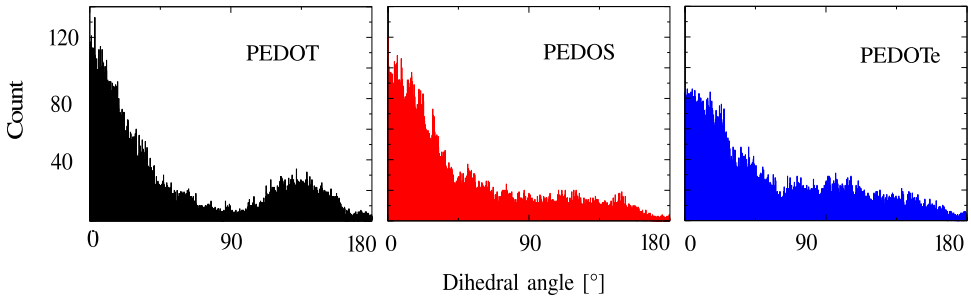

Fig. 3. (Color online) Dihedral angle distributions for PEDOT (black), PEDOS (red), and PEDOTe (blue).

note that the computed bond lengths do not indicate complete aromaticity. Our computed ground-state bond lengths for PEDOT and PEDOS agree closely with previously published results using other computational methods.[10,13] For the PEDOTe system, no previous simulations results appear to have been published.

The pentacycle geometry around the heteroatom is also of interest in these systems. The size of the heteroatom should conceivably affect its bonding angle in the pentacycle. At 0 K, we compute this angle to be 92.1° for S, 91.5° for Se, and 87.9° for Te. At ambient temperature, our computed bonding angles are, on average, 92°, 89°, and 85°, respectively (standard deviation 2° in all cases). Clearly, the angle at ambient temperature is essentially the same as in the ground state, with a possible tendency toward becoming slightly less sharp. Also, the results indicate that the angle becomes sharper the larger the heteroatom is, as expected.

The dihedral angle is the twisting angle between two consecutive monomers. In the ground state, the polymer is flat, with the pentacycles pointing in opposite directions for consecutive monomers. We here define the dihedral angle to be zero for the ground state. We also define *trans*-positioning as a configuration with a dihedral angle less than 90°, and *cis*-positioning as a configuration with a dihedral angle larger than 90°.

Figure 3 shows the dihedral angle distribution at ambient temperature. We see that for all three polymers, there is substantial twisting so that the polymers are, in general, no longer flat. Inspection of the histograms suggest that PEDOT has the highest count of small-angle *trans*-positioning of the three. Furthermore, the distribution for PEDOT has a second local maximum around 45° away from complete *cis*-positioning. Such a feature is missing for both PEDOS and PEDOTe. The heavier the heteroatom, the more spread out the dihedral angle distribution appears to be. Interestingly, twisting angle calculations[15–17] at 0 K find the twisting stiffness to be slightly higher for PEDOS compared to PEDOT. To further quantify the dihedral angle distribution, we calculated the average planarity $P = (||\theta| - 90|)/90$, where θ is the dihedral angle in degrees.[18] We find that the planarity decreases with increased atomic number of the heteroatom: $P = 0.67$ for PEDOT, 0.65 for PEDOS, and 0.59 for PEDOTe.

To further analyze these systems, we calculated point charges of selected atoms using the restrained electrostatic potential method,[14] both at 0 K and ambient temperature. The results for ambient temperature are statistical averages over the configurations obtained during the simulation.

Figure 4 shows the computed point charges on the carbon backbones of the six central monomers, as well as the point charges on the corresponding heteroatoms. For all three systems, the net charge on the heteroatom (S, Se, Te) is negative, becoming increasingly negative the heavier the heteroatom is.

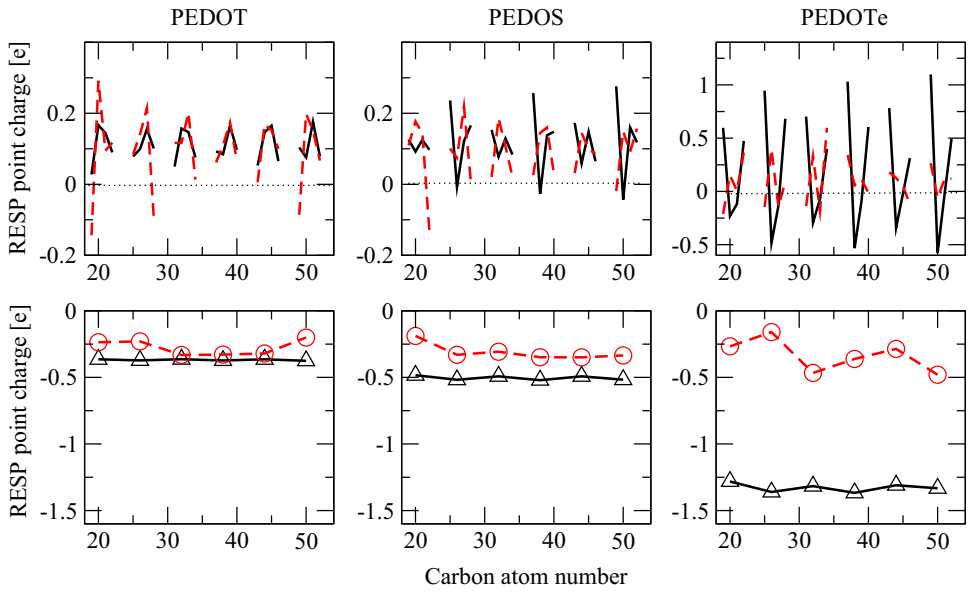

Fig. 4. (Color online) Point charges, expressed in units of the elementary positive charge *e*, on selected atoms on monomers 4–9 calculated using the restrained electrostatic potential (RESP) method. Upper row carbon backbone at 0 K (black full lines) and at 300 K (red dashed lines). Lower row heteroatoms (S, Se, Te) at 0 K (black full lines with triangles) and at 300 K (red dashed lines with circles). Values larger than zero imply a positive net charge, i.e., an electron deficit.

Comparing the results for 0 K and 300 K, we also see that the heteroatom point charge becomes less negative with increased temperature. In contrast, the atoms on the carbon backbones have, on average, positive point charges, except for PEDOTe where approximately equal numbers of positive and negative point charges are found. Also, the average point charge on the carbon backbone atoms appears to be essentially the same for both temperatures for all systems. The results for PEDOTe stand out from the other ones in that the fluctuations in the carbon backbone point charges are much larger than for the other two systems with lighter heteroatoms. The observed distributions of point charges over the carbon backbone in each monomer allow us to draw conclusions regarding the aromaticity of the systems. For PEDOT, the atoms 2 and 3 in the carbon backbone (see Fig. 1) have higher charge than atoms 1 and 4. This suggests an aromatic character. PEDOS shows a similar distribution for 300 K, with a partial switch to a more quinoid character at 0 K with atoms 1 and 4 in the carbon backbone now showing higher point charges than atoms 2 and 3. For PEDOTe, the character at 300 K appears to be intermediate between aromatic and quinoid conformations. At 0 K, however, the point charge profile suggests a quinoid character.

Finally, we also briefly discuss our computed energy gaps between the highest occupied molecular orbital (HOMO) the and lowest unoccupied molecular orbital (LUMO). Our calculated gaps are 1.21 eV for PEDOT, 1.15 eV for PEDOS and 1.00 eV for PEDOTe. The experimentally determined gaps for PEDOT and PEDOS are 1.6 eV and 1.4 eV, respectively.[19] Due to the discontinuity of the exchange–correlation potential, the Kohn–Sham one-electron band gap is usually underestimated in regular DFT calculations, and this is apparently also the case in the present work. However, our calculations do reproduce the experimentally observed trend, i.e., that the gap in the selenium derivative is smaller than the gap in PEDOT. Our calculations also predict that this trend persists in the tellurium derivative, as expected. For further comparison, we mention that Patra et al.[19] computed the gap in PEDOT to be 1.84 eV and PEDOS 1.66 eV using B3LYP.

CONCLUSIONS

In conclusion, our simulations at ambient temperature reveal an interesting behavior of the *cis*-positioned dihedral angle distribution for PEDOT in that there is a relative accumulation into a distinct local maximum in comparison to PEDOS and PEDOTe, where the corresponding distributions are more evenly spread out. Furthermore, aromaticity appears to be dominant for all three systems in the studied temperature range. The difference between long and short bond lengths is largest in PEDOTe, suggesting higher aromaticity. On the other hand, our analysis using point charges suggests that PEDOTe at low temperature may have a slightly more quinoid character compared to the other studied cases. The presence of solvents and dopants may conceivably alter the behavior of the polymers in significant ways. The formation of polarons affect the interatomic distances and may also alter the dihedral angle stiffness. Consideration of such issues is the subject of ongoing work.

ACKNOWLEDGEMENTS

The authors acknowledge financial support from Vetenskapsrådet (VR), The Royal Swedish Academy of Sciences (KVA), the Knut and Alice Wallenberg Foundation (KAW), Carl Tryggers Stiftelse (CTS), Swedish Energy Agency (STEM), Swedish Foundation for Strategic Research (SSF), and Erasmus Mundus Action 2 TARGET II consortium. We are grateful to Prof. Mathieu Linares for interesting scientific discussions and valuable suggestions. The computations were performed on resources provided by the Swedish National Infrastructure for Computing (SNIC) at the National Supercomputer Center (NSC), Linköping University, the PDC Centre for High Performance Computing (PDC-HPC), KTH, and the High Performance Computing Center North (HPC2N), Umeå University.

REFERENCES

1. O. Bubnova, Z.U. Khan, A. Malti, S. Braun, M. Fahlman, M. Berggren, and X. Crispin, *Nat. Mater.* (2011). doi:10.1038/nmat3012.
2. J. Luo, D. Billep, T. Waechtler, T. Otto, M. Toader, O. Gordan, E. Sheremet, J. Martin, M. Hietschold, D.R.T. Zahn, and T. Gessner, *J. Mat. Chem. A* (2013). doi:10.1039/C3TA11209H.
3. E.J. Bae, Y.H. Kang, K.-S. Jang, and S.Y. Cho, *Sci. Rep.* (2016). doi:10.1038/srep18805.
4. K. Ando, S. Watanabe, S. Mooser, E. Saitoh, and H. Sirringhaus, *Nat. Mater.* (2013). doi:10.1038/nmat3634.
5. R. Car and M. Parrinello, *Phys. Rev. Lett.* (1985). doi:10.1103/PhysRevLett.55.2471.
6. CPMD, Copyright IBM Corp (1990-2015), Copyright MPI für Festkörperforschung Stuttgart (1997–2001). http://www.cpmd.org/. Accessed 7 Nov 2016.
7. A.D. Becke, *Phys. Rev. A* (1988). doi:10.1103/PhysRevA.38.3098.
8. C. Lee, W. Yang, and R.G. Parr, *Phys. Rev. B* (1988). doi:10.1103/PhysRevB.37.785.
9. N. Troullier and J.L. Martins, *Phys. Rev. B* (1991). doi:10.1103/PhysRevB.43.1993.
10. E.-G. Kim and J.-L. Brédas, *J. Am. Chem. Soc.* (2008). doi:10.1021/ja806389b.
11. S. Nosé, *Mol. Phys.* (1984). doi:10.1080/00268978400101201.
12. W.G. Hoover, *Phys. Rev. A* (1985). doi:10.1103/PhysRevA.31.1695.
13. Y.H. Wijsboom, A. Patra, S.S. Zade, Y. Sheynin, M. Li, L.J.W. Shimon, and M. Bendikov, *Angew. Chem. Int. Ed.* (2009). doi:10.1002/anie.200901231.
14. C.I. Bayly, P. Cieplak, W. Cornell, and P.A. Kollman, *J. Phys. Chem.* (1993). doi:10.1021/j100142a004.
15. S. Das and S.S. Zade, *Chem. Commun.* (2010). doi:10.1039/B915826J.
16. A. Patra, M. Bendikov, and S. Chand, *Acc. Chem. Res.* (2014). doi:10.1021/ar4002284.
17. S.S. Zade, N. Zamoshchik, and M. Bendikov, *Acc. Chem. Res.* (2011). doi:10.1021/ar1000555.
18. J. Sjöqvist, J. Maria, R.A. Simon, M. Linares, P. Norman, K.P.R. Nilsson, and M. Lindgren, *J. Phys. Chem. A* (2014). doi:10.1021/jp506797j.
19. A. Patra, Y.H. Wijsboom, S.S. Zade, M. Li, Y. Sheynin, G. Leitus, and M. Bendikov, *J. Am. Chem. Soc.* (2008). doi:10.1021/ja8018675.